

Universality for Three Bosons with Large, Negative Effective Range: Aspects and Addenda

Harald W. Griesshammer ^{1*}

^{1*}Institute for Nuclear Studies, Department of Physics, The George Washington University, Washington DC, 20052, USA.

Corresponding author(s). E-mail(s): hgrie@gwu.edu;

Abstract

Resummed-Range Effective Field Theory is the consistent non-relativistic Effective Field Theory of point interactions in systems with large two-body scattering length a and an effective range r_0 large in magnitude but negative. Its leading order is non-perturbative, and its observables depend only on the dimensionless ratio $\xi := 2r_0/a$ once $|r_0|$ is chosen as base unit. This presentation highlights aspects for three identical spinless bosons and adds details to a previous discussion [1]. At leading order, no three-body interaction is needed. A ground state exists only in the range $0.366\dots \geq \xi \geq -8.72\dots$, and excited states display self-similarity and Discrete Scale Invariance, with small corrections for nonzero r_0 .

Keywords: Universality, Efimov effect, three bosons, large scattering length, large effective range, negative effective range, discrete scale invariance, three body interaction

1 Introduction

Two-body systems with shallow poles and effective ranges which are large in magnitude and negative occur most likely when $k \cot \delta$ has a large and negative curvature, typically induced by a resonance just above zero momentum, like in narrow Feshbach resonances, the $D_s^*(2317)$ and some ΞN and $\Xi \Xi$ systems [2–7]. Habashi and collaborators [8–10] studied such two-body systems by formulating a consistent non-relativistic Effective Field Theory (EFT) of one momentum-independent and one momentum-dependent contact interaction between two identical spinless bosons. This presentation

discusses some aspects of the cornucopia of universal scaling properties in its *three*-boson sector, adding material to a comprehensive study [1], which also contains a fuller list of references.

2 A Digest of the Formalism

Consider a system of two identical spinless, non-relativistic bosons which are characterised by a scattering length a and effective range r_0 . Once $|r_0|$ is chosen as base unit for distances and momenta, its observables are universal in the sense that they depend only on the dimensionless ratio

$$\xi := \frac{2r_0}{a} . \quad (1)$$

In the usual version called ‘‘Short-Range EFT’’, one considers $|r_0| \ll |a|$ ($\xi \rightarrow 0$) as perturbation and needs a stabilising three-boson (3B) interaction at leading order, leading to Efimov’s Discrete Scale Invariance [11–14]; see *e.g.* ref. [15] for a recent review. Here, we consider ‘‘Resummed-Range Effective Field Theory’’, the extension of Short-Range EFT to include large, and hence non-perturbative, ξ . In the 2B sector, its leading order is of course still non-perturbative, and the two interactions are tuned to reproduce both a large scattering length a and an effective range $r_0 < 0$ large in magnitude but negative [8–10]. The theory is also renormalisable provided the effective range is negative so that the Wigner bound is satisfied [16–19]:

$$r_0 < 0 . \quad (2)$$

Its leading-order 2B S -matrix takes the ‘‘second-simplest’’ non-trivial form,

$$S = \frac{K + i\kappa_2^-}{K - i\kappa_2^-} \frac{K + i\kappa_2^+}{K - i\kappa_2^+} , \quad (3)$$

characterised by exactly two poles with positions $i\kappa_2^\pm$ in the complex momentum plane:

$$\kappa_2^\mp := - \left[1 \mp \sqrt{1 - \xi} \right] \xrightarrow[\text{un-scale}]{r_0 \ll a \ (\xi \rightarrow 0)} \left(\frac{1}{a}, -\frac{2}{|r_0|} \right) . \quad (4)$$

[This equation includes the Short-Range EFT limit in un-rescaled variables, in which one pole becomes shallow, the other one deep.] Their evolution from one bound and one virtual state at $\xi < 0$ to a resonance for $\xi > 1$ is shown in fig. 1.

In the 3B system, the leading order is of course still nonperturbative. The corresponding Faddeev equation is shown in fig. 2. The j th bound state at momentum $i\kappa_3^{(j)}$ is the nontrivial solution to its homogeneous part with S -wave kernel

$$\mathcal{K}(-(\kappa_3^{(j)})^2; P, Q) := \frac{Q}{P} \frac{\ln \frac{P^2 + Q^2 + PQ + (\kappa_3^{(j)})^2}{P^2 + Q^2 - PQ + (\kappa_3^{(j)})^2}}{\xi + \frac{3Q^2 + 4(\kappa_3^{(j)})^2}{4} + \sqrt{3Q^2 + 4(\kappa_3^{(j)})^2}} . \quad (5)$$

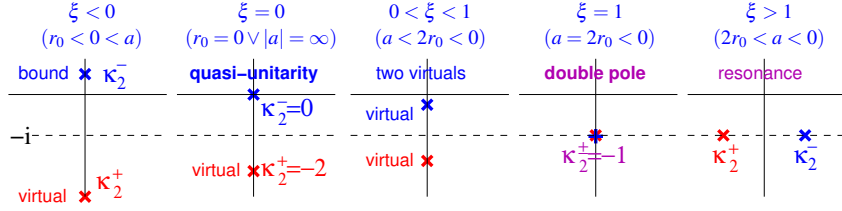


Fig. 1 (Colour on-line) 2B poles in the complex momentum plane as ξ (κ_2^-) increases (decreases).

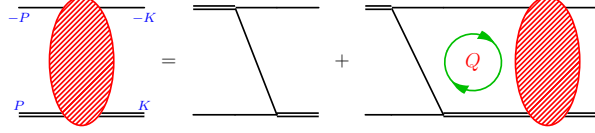


Fig. 2 (Colour on-line) Diagram of the 3B Faddeev integral equation. Double line: 2B amplitude.

As a practical matter, one discretises the kernel and scans in the (rescaled) “binding energy” $(\kappa_3^{(j)})^2 > 0$ for solutions of

$$\det[1 - \mathcal{K}(-(\kappa_3^{(j)})^2; P, Q)] = 0 \quad , \quad (6)$$

on a mesh which weighs low momenta more than higher ones. For example,

$$P, Q = (e^{zP, Q} - 1) \kappa_2^- (\xi - \epsilon) \quad (7)$$

with $\epsilon \approx \pm 10^{-[5\dots 7]}$ renders robust results of high accuracy quickly on grids of between 500 and 2000 points over a wide range of “hard” cutoffs $\Lambda \in [0.5; 3000]|r_0^{-1}|$.

3 A Curated Selection of Results

Figure 3 shows the central result: the binding momenta $i\kappa_3$ for the ground and first three excited states of the 3B system display what looks by eye to be self-similarity and Discrete Scale Invariance similar to that found in the Efimov effect of Short-Range EFT. However, upon closer inspection, small difference surface. The ground state’s binding momentum at threshold is with $\kappa_{\text{thr}}^{(0)} \approx 2.12 |r_0^{-1}|$ about 30% smaller than for an Efimov trajectory with the same 3B binding momentum at $\xi = 0$, where it is about $3.31 |r_0^{-1}|$. The difference is still about 15% for the first excitation. At zero binding, the ground (first excited) state is about 30% (10%) further away than the Efimov case. Overall, trajectories of the ground state and first few excitations are shorter in κ_2^- than those of Efimov trajectories. And while the tower of states is infinitely high and deep in Short-Range EFT, no stably-bound state exists in Resummed-Range EFT outside the range $0.367\dots \geq \xi \geq -8.726\dots$ (namely $-0.204\dots \leq \kappa_2^- \leq 2.118\dots$), and excitations appear only for smaller $|\xi|$ ($|\kappa_2^-|$): There are no bound states at $\xi = -10$, one at $\xi = -1$, two at $\xi = -0.1$, three at $\xi = -0.01$, and four at $\xi = -0.0001$.

These findings are however not un-surprising after a look at the kernel, eq. (5). The loop momentum Q dominates the 2B propagator for $Q \gg \kappa_3, \xi$ and tames its UV limit

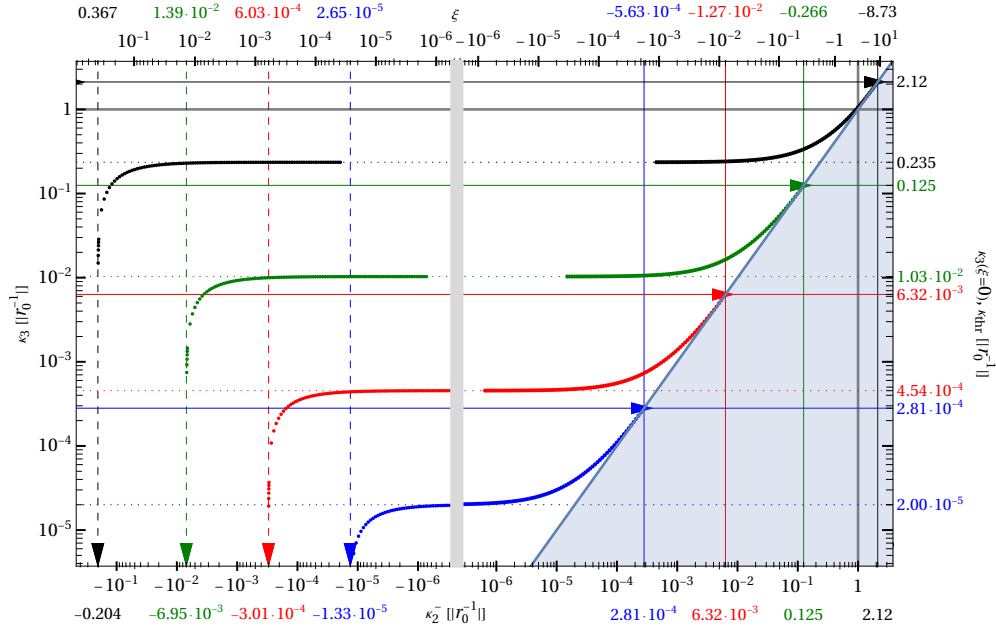


Fig. 3 (Colour on-line) Binding momenta κ_3 of the 3B system in $|r_0^{-1}|$ as function of the 2B binding momentum κ_2^- (bottom scale, in $|r_0^{-1}|$) and of ξ (top scale), for the ground state (black) and the 1st (green), 2nd (red) and 3rd (blue) excitations. Logarithmic scales on both axes, with positive and negative values in κ_2^- (ξ) stitched together by a gray line. Gray region: 3B state unstable, $\kappa_3 < \kappa_2^-$. Right axis: $\kappa_3^{(j)}$ at quasi-unity (dotted horizontal lines) and at threshold (solid horizontal and vertical lines). Top axis: ξ_{thr} at threshold and at zero-binding (dashed vertical lines). Bottom axis: corresponding κ_{thr} and $\kappa_{2\text{ZB}}$. Arrows point to zero binding (vertical), threshold (horizontal), and quasi-unity ($\kappa_{3\text{QU}}$, horizontal). All characteristic values are also found in table 1. The trajectory of the 3rd excitation is within line thickness indistinguishable from the one in Short-Range EFT with the same 3B binding momentum at quasi-unity.

so that a 3B interaction is not needed to stabilise the system against collapse. Since there are no external scales, no bound states emerge. At intermediate $\frac{3Q^2}{4} + \kappa_3^2 \gg \sqrt{3Q^2 + 4\kappa_3^2} \gtrsim 4$, the effective-range term $\frac{3Q^2}{4} + \kappa_3^2$ dominates over the unitarity term $\sqrt{3Q^2 + 4\kappa_3^2}$, and the integral still converges quickly. Since the binding momentum sets the scale of the loop momentum as $Q \lesssim \kappa_3$, bound states can be supported for $\kappa_3 \lesssim 2$. Indeed, the ground state's binding momentum $\kappa_3^{(0)} \leq 2.118\dots$ agrees with this estimate. For such states, effective-range effects are large since $|r_0| \sim a$ ($\xi \sim 1$).

Each bound state maps out a trajectory as function of ξ . At the **Threshold Point** $\kappa_{\text{thr}} := \kappa_3(\xi_{\text{thr}}) \stackrel{!}{=} \kappa_2^-(\xi_{\text{thr}})$, a 3B state emerges from the 2B continuum. As $0 > \xi > \xi_{\text{thr}}$ decreases in magnitude, both this 3B and all 2B sub-systems are bound, until the binding momentum of the shallowest 2B bound state vanishes at **Quasi-Unity** $\kappa_2^-(\xi = 0) = 0$, namely infinite 2B scattering length. Nonetheless, the 3B state remains bound there, $\kappa_{3\text{QU}} := \kappa_3(\xi = 0) > 0$. As $\xi \rightarrow 0$ (and hence the effective range $r_0 \rightarrow 0$) becomes perturbative around this point, $\frac{3Q^2}{4} + \kappa_3^2 \ll \sqrt{3Q^2 + 4\kappa_3^2}$ and the leading contribution becomes identical to Efimov's Short-Range EFT. This predicts that a

self-similar tower of Efimov states appears in which neighbouring trajectories obey “Efimov rescaling”, characterised by the transcendental number $s_0 = 1.0062378\dots$:

$$\lim_{j \rightarrow \infty} \left(\frac{\kappa_3^{(j)}(\kappa_2^-)}{\kappa_3^{(j+1)}(e^{\pi/s_0} \kappa_2^-)}, \frac{\kappa_{3\text{QU}}^{(j)}}{\kappa_{3\text{QU}}^{(j+1)}}, \frac{\kappa_{2\text{ZB}}^{-(j)}}{\kappa_{2\text{ZB}}^{-(j+1)}}, \frac{\kappa_{\text{thr}}^{(j)}}{\kappa_{\text{thr}}^{(j+1)}} \right) = e^{\pi/s_0} = 22.6944\dots \quad (8)$$

However, there is no need for a 3B interaction since the binding momentum $\kappa_2^+(\xi \rightarrow 0) \rightarrow -2 [|r_0|]$ of the second, virtual 2B state continues to provide a 2B scale for the 3B system’s binding momentum $\kappa_{3\text{QU}} := \kappa_3(\xi = 0) > 0$. Since a natural scale persists there, the system is only called close to “*quasi*-unitarity”. It is from that régime that the overall graph inherits a semblance of self-similarity.

As ξ turns positive, one proceeds in the Borromean region of a state’s trajectory, where the 3B system continues to be bound albeit all 2B subsystems are unbound (*i.e.* $\kappa_2^\pm < 0$ virtual). 3B binding continues to decrease until finally, the 3B system itself becomes unbound at **Zero Binding** $\kappa_3(\xi_{\text{ZB}}) = 0$ for $\kappa_{2\text{ZB}}^- := \kappa_2^-(\xi_{\text{ZB}}) < 0$.

Table 1 contains the binding momenta of the ground state and first three excitations at the three characteristic points. All these approach “Efimov scaling”, eq. (8), and the last row indeed infers universal constants of binding momenta for highly excited states. Numerical and extrapolation uncertainties are detailed in ref. [1].

Table 1 Characteristics of crucial points on the three-body trajectory: zero binding, quasi-unitarity and threshold. Values are given for the ground state and first three excitations as marked also in fig. 3, plus extrapolations for Efimov-like states. Uncertainties combine extrapolation and numerics.

state	zero binding $\kappa_2^-(\kappa_3 = 0) [r_0^{-1}]$	quasi-unitarity $\kappa_3(\kappa_2^- = 0) [r_0^{-1}]$	threshold $\kappa_3 \stackrel{!}{=} \kappa_2^- [r_0^{-1}]$
ground	$-2.04318(6) \cdot 10^{-1}$	$2.35412(3) \cdot 10^{-1}$	$2.11862(2)$
1st exc.	$-6.9517(5) \cdot 10^{-3}$	$1.03030(5) \cdot 10^{-2}$	$1.25108(1) \cdot 10^{-1}$
2nd exc.	$-3.0144(1) \cdot 10^{-4}$	$4.53987(1) \cdot 10^{-4}$	$6.320(1) \cdot 10^{-3}$
3rd exc.	$-1.3269(2) \cdot 10^{-5}$	$2.00039(5) \cdot 10^{-5}$	$2.810(3) \cdot 10^{-4}$
$j \rightarrow \infty$	$-0.1551(1) e^{-j \frac{\pi}{s_0}}$	$0.23381(8) e^{-j \frac{\pi}{s_0}}$	$3.31(2) e^{-j \frac{\pi}{s_0}}$

Figure 4 shows the dependence of the binding momenta on the cutoff employed to solve eq. (6), confirming that the system is indeed renormalised (*i.e.* insensitive to sort-distance Physics) *without* a stabilising 3B interaction. Notice that the cutoff variation spans more than two “Efimov cycles”, $\Lambda_{\text{max}}/\Lambda_{\text{min}} \approx 6000 \approx (e^{\pi/s_0})^{2.8}$.

Figure 5 shows that it is quite unlikely that more-deeply bound states exist, supporting the argument above. Its two graphs explore zeroes of the kernel’s determinant (6): the left one at quasi-unitarity $\kappa_2^- = \xi = 0$ (vertical gray line in fig. 3), the right one on a parallel to the threshold parametrised by $\kappa_2^- = 0.9\kappa_3$. Both explore more than two “Efimov cycles”, $\kappa_{3\text{max}}/\kappa_{3\text{min}} \approx 1000 \approx (e^{\pi/s_0})^{2.2}$. Both determinants approach unity for large putative κ_3 , with no indication of a turn-around. The trained eye will discern that what looks like a line is actually a dense set of points at which the determinant is sampled.

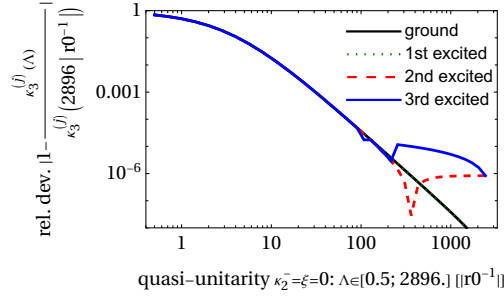


Fig. 4 (Colour on-line) Dependence of the binding momenta of the ground and first three excited states at quasi-unity on the cutoff of the integral equation eq. (6). For all states, the result at $\Lambda \approx 10|r_0|$ differs from the asymptotic one by $\lesssim 1\%$. At a relative accuracy of 10^{-5} , numerical instabilities enter for the second and third excitation.

While scaling is already approximately seen in fig. 3, it becomes more transparent when the trajectory of the j th bound state is normalised to its value at threshold,

$$\mathcal{R}^{(j)} \left(x_\kappa := \frac{\kappa_2^-}{\kappa_{\text{thr}}^{(j)}} \right) := \frac{\kappa_3^{(j)}}{\kappa_{\text{thr}}^{(j)}}, \quad (9)$$

and expressed as function of the rescaling variable x_κ with $\mathcal{R}^{(j)}(x_\kappa = 1) \stackrel{!}{=} 1$. Inspired by Efimov's universal function $\Delta(\xi)$ [12–14], one transforms in addition from Cartesian coordinates in the $(x_\kappa, \mathcal{R}^{(j)}(x_\kappa))$ plane to polar ones,

$$\begin{aligned} x_\kappa &= \sqrt{2} \rho^{(j)}(\theta) \cos\left(\theta + \frac{\pi}{4}\right), \\ \mathcal{R}^{(j)}(x_\kappa) &= \sqrt{2} \rho^{(j)}(\theta) \sin\left(\theta + \frac{\pi}{4}\right). \end{aligned} \quad (10)$$

The threshold is then normalised to $\rho(\theta = 0) = 1$, quasi-unity is at $\theta = \frac{\pi}{4}$, and zero binding at $\theta = \frac{3\pi}{4}$. Using an idea by Gattobigio *et al.* [20], the trajectories are in

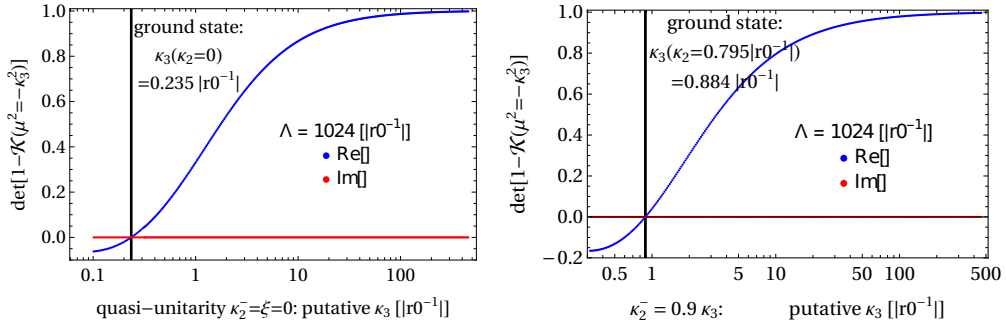


Fig. 5 (Colour on-line) Determinant of the bound-state kernel, eq. (5), at putative values of κ_3 with fixed $\kappa_2^- = 0$ (left; quasi-unity) and $\kappa_3 = \kappa_2^-/0.9$ (right, parallel to threshold line). The dense κ_3 distribution appears to be a line. There are no zeroes after $\kappa_3^{(0)}(\kappa_2^- = 0) = 0.235 \dots |r_0|$ (left) and $\kappa_3^{(0)}(\kappa_2^- = 0.9\kappa_3) = 0.884 \dots |r_0|$ (right), indicating the absence of more-deeply bound 3B states.

this form parametrised with residuals of $\ll 10^{-3}$ by the 7 constants of table 2 via

$$\rho_{\text{param}}^{(j)}(\theta) = \exp\left(\sum_{n=1}^7 c_n^{(j)} \theta^{n/2}\right). \quad (11)$$

Table 2 The highly correlated ($|c_n, c_m| > 0.6$) coefficients of $\rho_{\text{param}}^{(j)}$ of state j in eq. (11), in $\text{rad}^{-n/2}$. The 68% confidence interval for a prediction at a single, new θ is $\rho_{\text{param}}^{(j)}(\theta) \pm w_{\text{pred}}^{(j)}$.

state	$c_1^{(j)}$	$c_2^{(j)}$	$c_3^{(j)}$	$c_4^{(j)}$	$c_5^{(j)}$	$c_6^{(j)}$	$c_7^{(j)}$	$w_{\text{pred}}^{(j)}$
$j = 0$	-4.7545	4.3710	-7.4404	11.714	-11.0015	5.54726	-1.12595	0.00009
$j = 1$	-4.2764	1.0734	-1.6005	5.4777	-6.58104	3.64577	-0.768214	0.00003
$j = 2$	-4.6823	1.4352	-1.2221	4.1199	-5.08001	2.87318	-0.613720	0.00003
$j = 3$	-4.7003	1.1952	0.014514	1.5657	-2.44535	1.53708	-0.348975	0.00011

In this parametrisation shown in fig. 6, one clearly sees that a large effective range (*i.e.* large ξ) has indeed the biggest impact on the ground state, while its effect on higher excitations decreases. The second and third excitation's trajectories are practically indistinguishable from each other, and either can be taken to represent an ‘‘Efimov’’ trajectory in Short-Range EFT with the same $\kappa_{3\text{QU}}$.

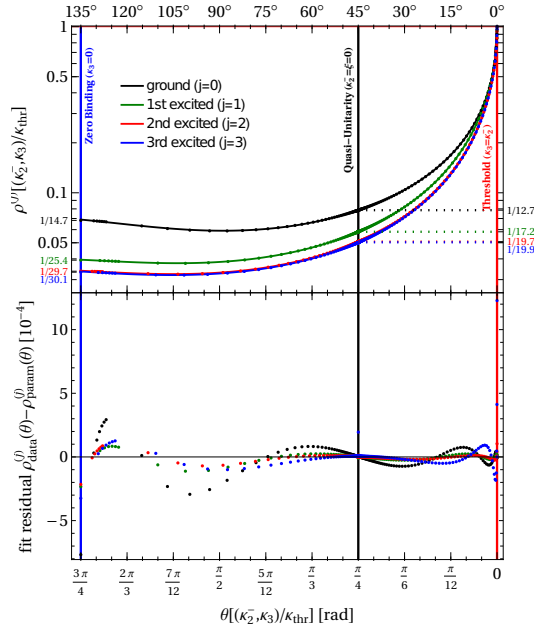


Fig. 6 (Colour on-line) Top: Data and fit of trajectories of the ground state and first three excitations in polar form, eq. (10), in a linear-log plot. The intra-trajectory ratios $\kappa_{3\text{QU}}^{(j)}/(\sqrt{2}\kappa_{\text{thr}}^{(j)})$ and $|\kappa_{2\text{ZB}}^{-(j)}/(\sqrt{2}\kappa_{\text{thr}}^{(j)})|$ are marked on the right and left, respectively. To facilitate comparison with fig. 3, θ increases from threshold (right) to the left. Bottom: Fit residuals on a linear scale, rescaled by 10^4 .

This similarity also explains that within each trajectory, the ratios between $\kappa_3^{(j)}$ at zero binding and threshold, and between quasi-unitarity and threshold, approach the Efimov-scaling predictions of Short-Range EFT; see values on the axes of fig. 6.

However, there is an important difference. In Resummed-Range EFT, a 3B interaction is needed to stabilise the system. By dimensional transmutation, this renormalisation leads to a dimensionful scale parameter Λ_* which fixes the position of the Efimov tower of 3B states, but whose value may differ in different systems since this theory has at leading order no knowledge of r_0 . In contradistinction, the position of the tower is in Resummed-Range EFT a parameter-free prediction once the positions of the two 2B poles are determined. This different behaviour of the two EFTs is, of course, a consequence of the fact that Short-Range EFT has no remaining natural scale once the 2B binding is zero, while the second pole at $\kappa_2^+ = -2$ still provides one in Resummed-Range EFT. Therefore, Resummed-Range EFT can be interpreted as an underlying theory to Short-Range EFT. It *predicts* Λ_* in units of $|r_0^{-1}|$ for $r_0 < 0$ when one matches the 3B binding momentum of the same state in the two versions at quasi-unitarity. This value (in regularisation with a “hard” cutoff) is actually near-identical for all states, with a less-than 1% deviation even for the ground state:

$$\Lambda_*^{(j \geq 2)} = 0.610206(1) |r_0^{-1}| . \quad (12)$$

4 Conclusion

In Resummed-Range EFT, properties of few-body systems are determined by two parameters: the two-body effective range r_0 and the dimensionless ratio $\xi = 2r_0/a$, where a is the 2B scattering length. As long as $r_0 < 0$, this EFT is self-consistent and renormalisable at leading order without a three-body interaction. While its spectrum appears at first glance quite self-similar and close to a truncated Efimov spectrum, noticeable ξ -dependence exists for the ground state and lowest excitations. Still, the spectrum approaches Efimov’s exact Discrete Scale Invariance for higher excitations.

If Short-Range EFT is interpreted as low-energy version of Resummed-Range EFT, then the absolute position of the Efimov tower is fixed, and the corresponding Efimov scale is $\Lambda_* = 0.610206(1) |r_0^{-1}|$ (in a renormalisation scheme with “hard” cutoff regularisation); see eq. (12). It will be quite interesting to put this prediction to the test in systems where Resummed-Range EFT applies.

Further details about these findings and results on scattering a boson on a bound 2B state in Resummed-Range EFT can be found in ref. [1]. The fate of the 3B trajectory in the sub-threshold and unbound regions will be discussed in future publications [21]. Obvious extensions include systems of three identical fermions; bosons with different masses; more than three particles; and higher-order effects, *e.g.* from a 2B shape parameter. Finally, the predictions (with truncation estimates from higher-order effects) should be confronted with data of suitable systems in Atomic, Nuclear and Particle Physics which are characterised by a large but negative effective two-body effective range and a large-in-magnitude scattering length.

Acknowledgements. It continues to be a pleasure to collaborate with Ubirajara van Kolck. I am grateful to the organisers and participants of EuroFewB 2023 in Mainz

for spirited, stimulating and profound discussions, a delightful atmosphere, and for indulging such a topic as the last plenary presentation. Instrumental for this research were the warm hospitality and financial support for stays at IJCLab Orsay and at the Kavli Institute for Theoretical Physics which is supported in part by the National Science Foundation under Grant No. NSF PHY-1748958. This material is based upon work supported in part by the U.S. Department of Energy, Office of Science, Office of Nuclear Physics, under award DE-SC0015393.

Author Contributions

The single author contributed all of the effort to this presentation, and none more. hg.

Data Availability Statement

All data underlying this work are available in full upon request from the author.

Competing Interests

The author declares no competing interests.

References

- [1] H. W. Griesshammer and U. van Kolck, *Eur. Phys. J. A* **59** (2023) 289 doi:[10.1140/epja/s10050-023-01196-0](https://doi.org/10.1140/epja/s10050-023-01196-0) [[arXiv:2308.01394](https://arxiv.org/abs/2308.01394)] [[nucl-th](#)].
- [2] J. van de Kraats, D. J. M. Ahmed-Braun, J. L. Li and S. J. J. M. F. Kokkelmans, *Phys. Rev. A* **107** (2023) 023301 doi:[10.1103/PhysRevA.107.023301](https://doi.org/10.1103/PhysRevA.107.023301) [[arXiv:2210.14200](https://arxiv.org/abs/2210.14200)] [[cond-mat.quant-gas](#)].
- [3] D. S. Petrov, *Phys. Rev. Lett.* **93** (2004) 143201 doi:[10.1103/PhysRevLett.93.143201](https://doi.org/10.1103/PhysRevLett.93.143201) [[cond-mat/0404036](#)] [[cond-mat.stat-mech](#)].
- [4] I. Matuschek, V. Baru, F.-K. Guo and C. Hanhart, *Eur. Phys. J. A* **57** (2021) 101 doi:[10.1140/epja/s10050-021-00413-y](https://doi.org/10.1140/epja/s10050-021-00413-y) [[arXiv:2007.05329](https://arxiv.org/abs/2007.05329)] [[hep-ph](#)].
- [5] A. M. Gasparyan, J. Haidenbauer and C. Hanhart, *Phys. Rev. C* **85** (2012) 015204 doi:[10.1103/PhysRevC.85.015204](https://doi.org/10.1103/PhysRevC.85.015204) [[arXiv:1111.0513](https://arxiv.org/abs/1111.0513)] [[nucl-th](#)].
- [6] J. Haidenbauer, U.-G. Meißner and S. Petschauer, *Nucl. Phys. A* **954** (2016) 273 doi:[10.1016/j.nuclphysa.2016.01.006](https://doi.org/10.1016/j.nuclphysa.2016.01.006) [[arXiv:1511.05859](https://arxiv.org/abs/1511.05859)] [[nucl-th](#)].
- [7] J. Haidenbauer and U.-G. Meißner, *Phys. Lett. B* **829** (2022) 137074 doi:[10.1016/j.physletb.2022.137074](https://doi.org/10.1016/j.physletb.2022.137074) [[arXiv:2109.11794](https://arxiv.org/abs/2109.11794)] [[nucl-th](#)].
- [8] J. B. Habashi, S. Sen, S. Fleming and U. van Kolck, *Annals Phys.* **422** (2020) 168283 doi:[10.1016/j.aop.2020.168283](https://doi.org/10.1016/j.aop.2020.168283) [[arXiv:2007.07360](https://arxiv.org/abs/2007.07360)] [[nucl-th](#)].

- [9] J. B. Habashi, S. Fleming and U. van Kolck, *Eur. Phys. J. A* **57** (2021) 169 doi:[10.1140/epja/s10050-021-00452-5](https://doi.org/10.1140/epja/s10050-021-00452-5) [[arXiv:2012.14995](https://arxiv.org/abs/2012.14995) [hep-ph]].
- [10] U. van Kolck, *Symmetry* **14** (2022) 1884 doi:[10.3390/sym14091884](https://doi.org/10.3390/sym14091884) [[arXiv:2209.08432](https://arxiv.org/abs/2209.08432) [hep-ph]].
- [11] V. Efimov, *Phys. Lett. B* **33** (1970) 563 doi:[10.1016/0370-2693\(70\)90349-7](https://doi.org/10.1016/0370-2693(70)90349-7).
- [12] V. N. Efimov, *Sov. J. Nucl. Phys.* **12** (1971) 589.
- [13] V. Efimov, *Nucl. Phys. A* **210** (1973) 157 doi:[10.1016/0375-9474\(73\)90510-1](https://doi.org/10.1016/0375-9474(73)90510-1).
- [14] V. Efimov, *Sov. J. Nucl. Phys.* **29** (1979) 546.
- [15] H.-W. Hammer, S. König and U. van Kolck, *Rev. Mod. Phys.* **92** (2020) 025004 doi:[10.1103/RevModPhys.92.025004](https://doi.org/10.1103/RevModPhys.92.025004) [[arXiv:1906.12122](https://arxiv.org/abs/1906.12122) [nucl-th]].
- [16] D. R. Phillips, S. R. Beane and T. D. Cohen, *Annals Phys.* **263** (1998) 255 doi:[10.1006/aphy.1997.5771](https://doi.org/10.1006/aphy.1997.5771) [[hep-th/9706070](https://arxiv.org/abs/hep-th/9706070)].
- [17] S. R. Beane, T. D. Cohen and D. R. Phillips, *Nucl. Phys. A* **632** (1998) 445 doi:[10.1016/S0375-9474\(98\)00007-4](https://doi.org/10.1016/S0375-9474(98)00007-4) [[nucl-th/9709062](https://arxiv.org/abs/nucl-th/9709062)].
- [18] C. J. Fewster, *J. Phys. A* **28** (1995) 110 doi:[10.1088/0305-4470/28/4/031](https://doi.org/10.1088/0305-4470/28/4/031) [[hep-th/9412050](https://arxiv.org/abs/hep-th/9412050)].
- [19] D. R. Phillips and T. D. Cohen, *Phys. Lett. B* **390** (1997) 7 doi:[10.1016/S0370-2693\(96\)01411-6](https://doi.org/10.1016/S0370-2693(96)01411-6) [[nucl-th/9607048](https://arxiv.org/abs/nucl-th/9607048)].
- [20] M. Gattobigio, M. Göbel, H.-W. Hammer and A. Kievsky, *Few B. Syst.* **60** (2019) 40 doi:[10.1007/s00601-019-1504-1](https://doi.org/10.1007/s00601-019-1504-1) [[arXiv:1903.05493](https://arxiv.org/abs/1903.05493) [cond-mat.quant-gas]].
- [21] H. W. Griebhammer and U. van Kolck, in preparation.